Journal of Neuroscience Methods 195 (2011) 176–184

Contents lists available at ScienceDirect

Journal of Neuroscience Methods

journal homepage: www.elsevier.com/locate/jneumeth

Flexible parylene-based microelectrode arrays for high resolution EMG recordings in freely moving small animals

Cinzia Metallo[a,d,*], Robert D. White[b,d], Barry A. Trimmer[c,d]

[a] Neuroscience Program, Tufts University School of Medicine, Boston, MA, United States
[b] Mechanical Engineering Department, Tufts University, Medford, MA, United States
[c] Biology Department, Tufts University, Medford, MA, United States
[d] Advanced Technology Laboratory, Tufts University, Medford, MA, United States

ARTICLE INFO

Article history:
Received 16 August 2010
Received in revised form
30 November 2010
Accepted 1 December 2010

Keywords:
Flexible microelectrode array
Electrophysiology
Electromyography
Parylene C
Microfabrication
Soft-bodied animals
Small animals

ABSTRACT

We present the development, fabrication and *in vivo* testing of a minimally invasive microelectrode array intended for high resolution multichannel recordings of electromyographic (EMG) signals. Parylene C was chosen as the structural substrate for its mechanical, electrical and physical properties. In particular, the device is extremely flexible. This provides a highly conformal coverage of the muscle surface and, at the same time, some degree of strain relief against the forces of micro-motion between the electrode and the surrounding tissues. By flexing and shaping itself to the muscles, the array is capable of maintaining a more stable electrical contact resulting in a significantly improved signal to noise ratio (SNR). To yield high signal selectivity, the design of the microelectrode array has been custom tailored to match the muscle anatomy of a particular animal system, the tobacco hornworm *Manduca sexta*. However, using the same fabrication protocol but different design parameters, the microdevice presented here can be easily implemented to study motor control and motor coordination in a vast range of small animals.
© 2010 Elsevier B.V. All rights reserved.

1. Introduction

An important challenge in neuroscience is to understand how the neural commands produced by the central nervous system (CNS) control motor coordination (Chiel et al., 2009). Although the organizational principles of motor control are becoming better understood (Dickinson et al., 2000; Nishikawa et al., 2007), it is still not possible to replicate the range of animal locomotor performance (Kar, 2003). This is partly due to the fact that animals operate as integrated neuromechanical machines driven by muscles that are intrinsically complex and non-linear in both their electrical and mechanical responses (Marsh, 1999; Huxley, 2000). As a result, an electromyographic (EMG) signal is a convoluted signal (Gielen, 1999). The ability to extract fine-scale electrical information from it depends on the detection capabilities of the recording instrumentation. In particular, the spatiotemporal resolution of the recording electrodes must be sufficiently high to maximize the signal to noise ratio (SNR) and allow high signal selectivity (Reaz et al., 2006). In these past few years, technical advances in electronics and fabrication methods have prompted a steady advance in the design and manufacturing of EMG recording devices. Besides surface electromyography, inserting microwires directly into muscles has been by far the most common method to record muscle activity. Typically, two Teflon insulated platinum alloy fine wires are twisted together to form a bipolar electrode (De Luca, 2006). By differentially amplifying the voltage measured at the terminal ends of the two wires, noise fluctuations can be considerably reduced. To enhance the limited spatial sensitivity of this type of intramuscular recording, multiple microwire electrodes have been employed in many neurophysiological studies (Buchthal et al., 1957; Vitti and Basmajian, 1977; Jayne, 1988; Jayne and Lauder, 1995; Hillel, 2001).

More recently, microfabrication has marked a major step forward in the development of neural and EMG implants (Voldman et al., 1995; HajjHassan et al., 2008). The adaptability of the photolithography process, in fact, allows for the manufacturing of devices with customizable design parameters. By precisely controlling the size of the recording sites, their density, and their interspacing, it is possible to fine-tune performance characteristics such as electrode impedance, signal discrimination, and signal sensitivity. Low profile devices with anatomically conforming properties also facilitate subcutaneous insertion and positioning. Furthermore, the availability of a large number of recording sites arranged in specific geometries offer the possibility to sample wider muscle areas – if not different muscles – and eventually monitor

* Corresponding author at: Advanced Technology Laboratory, Tufts University, 200 Boston Avenue, Suite 2600, Medford, MA 02155, United States.
Tel.: +1 617 627 0900; fax: +1 617 627 0909.
E-mail address: Cinzia.Metallo@tufts.edu (C. Metallo).

0165-0270/$ – see front matter © 2010 Elsevier B.V. All rights reserved.
doi:10.1016/j.jneumeth.2010.12.005

several motor units simultaneously. This is particularly important as multichannel EMG recordings are crucial for a more comprehensive functional-anatomical analysis of motor coordination (Ting and Macpherson, 2005; Lockhart and Ting, 2007).

One of the main limitations of many EMG devices is the intrinsic stiffness of the materials used as substrate (Subbaroyan et al., 2005). Silicon, for example, is extensively employed due to its well known electrical properties (Wise, 2005). The rigidity of silicon-based probes, however, represents a considerable problem for *in vivo* implantations. In fact, the mismatch between the mechanical properties of the stiff probe and the much softer surrounding tissues may result in tissue damage, tolerability issues, and micromotion of the electrodes with respect to the muscle. Consequent motion artifacts may significantly distort the recorded signal and complicate data analysis. One way to mitigate this problem is to select substrate materials according to a more suitable combination of their electrical and mechanical properties. Several flexible and biocompatible polymers, such as polyimide (Richardson et al., 1993), are being increasingly used (Farina et al., 2008). The flexibility of the resulting devices provides a more conformal coverage of the muscle surface and supplies some degree of strain relief against the forces of micro-motion. Since a more uniform electrical contact is established at the electrode-tissue interface, the SNR can be significantly improved.

Although considerable work has focused on the neuromuscular systems of vertebrates, invertebrates offer several advantages for understanding motor coordination and for developing high resolution EMG devices. One of the most important of these advantages is that each muscle is controlled by few neurons so the number of "information channels" that need to be monitored is small compared to most vertebrates (Clarac and Pearlstein, 2007). Furthermore, the small size of most invertebrates makes the simultaneous recording from multiple muscles an easier task and activation patterns can be more accurately matched to motor tasks. On the other hand, however, their size represents a significant challenge in manufacturing devices sufficiently small to be inserted without muscle damage. EMG recordings with multiple wire bipolar electrodes have been reported in freely behaving small animals (Ayers and Davis, 1977; Ahn and Full, 2002; Whelan, 2003; Ahn et al., 2006) but the need for multiple insertions coupled with inevitable wiring problems during the recording sessions constitute a substantial experimental limitation. To overcome these problems, the use of flexible micro-fabricated devices has been proposed to achieve multiunit EMG recordings (Spence et al., 2007). Here we present a flexible and minimally invasive parylene C-based microelectrode array intended for *in vivo* EMG acquisition in small insects. Due to its conformal coating, biocompatibility and moisture/chemical barrier properties, parylene C has been extensively used as insulation for biomedical probes (Loeb et al., 1977; Schmidt and McIntosh, 1988; Licari, 2003). However, it is only when parylene C is used as structural substrate that it is possible to take full advantage of its entire range of mechanical, electrical and physical properties (Rodger et al., 2008; Herold and Rasooly, 2009).

To ensure ease of insertion, optimal placement and recording stability, the geometry of any implantable electrode array intended to record EMGs in a living system must match the muscle anatomy of that system. For this reason, the design of our device was customized to record from muscles in a well characterized insect model, *Manduca sexta* (Levine and Truman, 1985; Belanger and Trimmer, 2000; Trimmer and Issberner, 2007). In the larval (caterpillar) stage, *Manduca* is predominantly soft-bodied with very few hard body parts. Unlike vertebrates, whose movements are based on muscles acting on a rigid skeleton via joints and tendons, soft-bodied organisms exhibit a much greater range of movements and are able to deform and orient their bodies in almost any available direction. Even though they represent the vast majority of the animal biomass, little is known about their motor control strategies. Commonly available EMG microwire electrodes have a relatively poor spatial resolution and their rigidity does not guarantee a normal behavioral response. More importantly, in soft-bodied animals, the problem of electrode micro-motion is exacerbated by the elevated difference in mechanical stiffness between the implant and the exceedingly softer surrounding tissues. The microfabricated device presented here offers the opportunity to overcome all these experimental limitations and may represent a valid new methodology for the study of motor coordination not only in soft animals, but also in a wide range of small animals.

2. Materials and methods

2.1. Material selection

Parylene C, a crystalline thermoplastic polymer, has been chosen as the structural substrate for our microelectrode array due to the unique combination of its physical, chemical and mechanical properties. The deposition process, based on vapor polymerization, ensures that parylene C films are, at the same time, highly conformal, uniform, and pinhole-free. In addition to its intrinsic flexibility and mechanical strength (tensile modulus 3.2 GPa), parylene C is also chemically inert, is not subject to hydrolytic degradation (water absorption 0.01% for 0.019 in. and 0.06% for 0.029 in. after 24 h; water vapor transmission rate 0.0004 ng/Pa s m^2 at 37 °C) (http://advancedcoating.com/techinfo/typical.html; Licari, 2003) and meets the highest biocompatibility standards for plastic materials (ISO 10993 and USP Class VI) (Herold and Rasooly, 2009). Furthermore, due to its low dielectric constant (~3.1 at 1 kHz) (Licari, 2003) parylene C is capable of minimizing the capacitive crosstalk between adjacent metal lines even when deposited in very thin layers. Finally, parylene is optically transparent, allowing tissues to be seen through the array and, therefore, facilitating the correct positioning of the device and the post-mortem evaluation of the probe location. Taken together, all these properties make parylene C exceptionally well-suited for use as a substrate material in the fabrication of devices for long term EMG recordings.For the electrode material, gold has been chosen due to its well documented biocompatibility and electrochemical stability.

2.2. Design parameters

The design of our flexible microelectrode array has been custom-tailored to the anatomical features of *M. sexta*, our animal system. The array consists of 8 circular recording electrodes, each with a radius of 50 μm. The diameter of the electrodes was chosen to match the range of widths of *Manduca* muscle fibers (Rheuben, 1992; Woods et al., 2008) to yield high signal selectivity. In this way, the array should be capable of resolving EMG signals in individual muscles with single fiber resolution. The longitudinal spacing between the electrodes was selected to distribute different recording sites on distinct fibers of the same muscle. A set of 3 longitudinal spacing values (500 μm, 750 μm, 1000 μm) has been evaluated to be sufficient to provide an accurate placement of the array on the vast majority of muscles. The transverse spacing between the electrodes defines the final width of the device and, therefore, determines the area of the muscle that is ultimately covered by the array. To guarantee an optimal coverage of most muscles, 4 widths were selected (700 μm, 1000 μm, 1200 μm, 1500 μm) and the electrode sites were distributed accordingly. Interconnecting traces are routed among the electrodes and terminate into 300 μm × 300 μm output pads with a pitch of 500 μm (Fig. 1A).

The front part of the probe ends in a sharp tip to facilitate the insertion process (Fig. 1B). Only a fraction of the total length

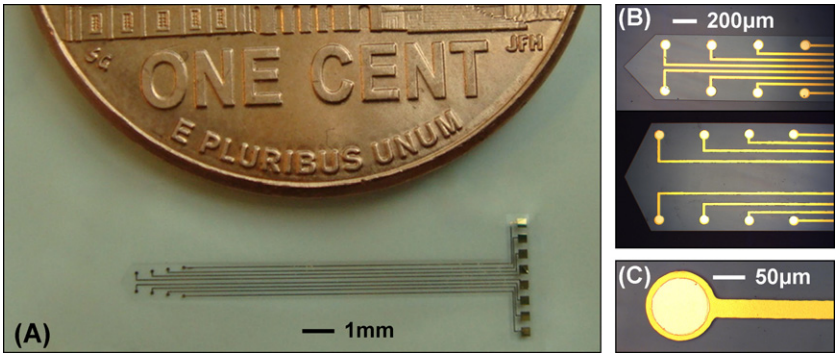

Fig. 1. Microfabricated device. (A) One of the microfabricated devices next to a US penny for size comparison. (B) Photomicrograph of two arrays with different transverse spacing values between the recording electrodes. (C) Photomicrograph of a single recording electrode showing the exposed gold pad (light yellow) and the parylene-insulated region (dark yellow). (For interpretation of the references to color in this figure legend, the reader is referred to the web version of the article.)

(3–5 mm) is intended to be inserted into the animal. The remaining part (1–2.5 cm) has been designed to allow some strain relief and yet maximize the number of devices that can be accommodated on a single wafer. Devices with short shanks are mainly used for EMG recordings in semi-intact preparations.

The overall thickness of the probe is another important design parameter and has been selected as a trade-off value between 3 key requirements: the device needs to be stiff enough to be inserted without buckling; it needs to be thin enough to slide easily between muscle fibers; and it needs to be flexible enough to preserve a stable and conformal coverage of the muscle surface. After a series of implantation experiments with parylene C films of different thicknesses, the ideal value has been evaluated to be in the range of 15–30 μm.

2.3. Fabrication methods

The fabrication protocol comprises a two mask photolithography process, vapor deposition of parylene C, sputtering deposition, and reactive ion etching. A schematic of the process flow is shown in Fig. 2. As a first step, approximately 15 μm of parylene C is vapor deposited from the monomer at room temperature and approximately 35 mT (Specialty Coating Systems, PDS 2010 Labcoter®2) on a ⟨1 0 0⟩ oriented, lightly boron doped, 100 mm diameter silicon wafer (Fig. 2A). This layer of parylene constitutes an optically transparent, flexible and insulating base for the devices, on top of which the metallic structures can be patterned. To shape the array geometry, 3 μm of positive photoresist (SPR 220-3.0 series) is spun over the parylene layer, exposed, and developed. Thin films of chromium (30 nm) and gold (300 nm) are then sputtered onto the wafer. The chromium layer is deposited to promote adhesion between parylene and gold. No additional adhesion treatment is required. Next, the wafer is sonicated in an acetone bath until the metal lifts off (Fig. 2B), delineating the geometry of the device (i.e. recording electrodes, conductive lines, and connection pads). A second insulating layer of parylene C (~1 μm) is then deposited on the whole wafer to encapsulate all the patterned metallic structures (Fig. 2C). Next, parylene is selectively removed only from the areas of the wafer corresponding to the recording sites and the connection pads, thereby leaving the conductive traces coated. First, a 3 μm photoresist layer is spun, exposed and developed. Next, a thin layer (150 nm) of copper is sputter deposited over the lift off pattern defined by photolithography. Once the photoresist is stripped in an acetone bath (Fig. 2D), the metal layer acts as an excellent etch mask and the wafer can be safely subjected to a reactive ion etch (March CS-1701F RIE) in oxygen plasma (100 sccm O_2, 280 mT, 200 W, etch rate 0.4 μm/min). The plasma etch is carried out until parylene is completely removed not only from the recording elec-

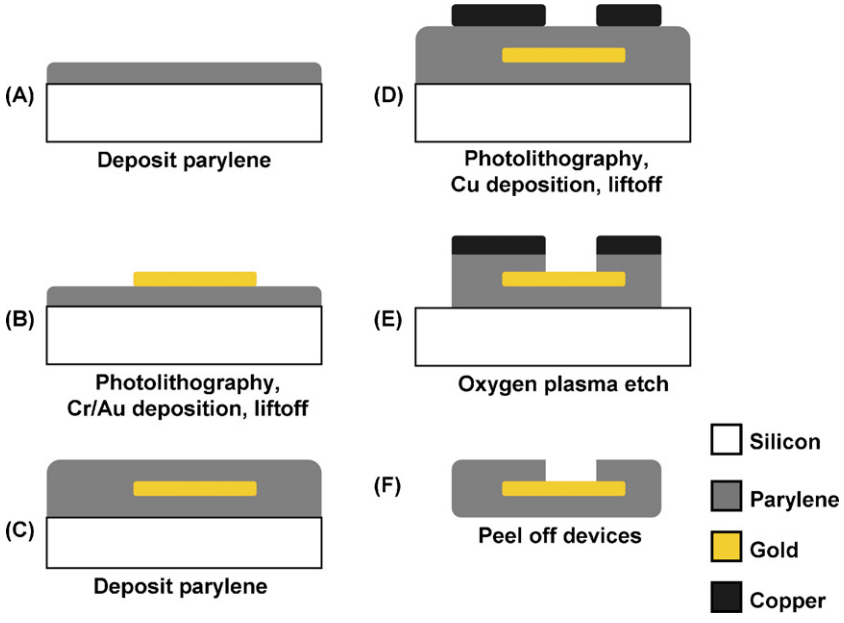

Fig. 2. Main fabrication steps. Main steps of the fabrication process. For a more detailed description, see Section 2.3.

trodes and the connection pads, but also from the area surrounding the devices to define their final shape (Fig. 2E). After a quick copper wet etch in standard acid metal etching chemistries, the devices are ready to be manually peeled off the wafer (Fig. 2F). No additional sacrificial release layer is needed; adhesion of the parylene to the silicon is sufficient for processing, but the devices can be manually peeled from the surface without damage.

2.4. Interconnect

To interface the fabricated microelectrode array with the recording instrumentation, the terminal end of the device has been designed to fit into the insertion slot of an 8 channel zero insertion force (ZIF) connector (Hirose, FH34S). To obtain both a reliable electrical and mechanical connection, cut-to-size masking tape is used as a stiffener to increase the thickness of the terminal end to approximately 0.3 mm. Once the device is inserted, a back-flip rotating actuator firmly holds it in place. After the actuator is locked, a visual inspection of the contacts is carried out with a microscope to ensure that the device is correctly positioned. The other end of the ZIF connector is soldered to a flat flex cable (Parlex series 050R08), which is inserted into another ZIF connector. This connector, in turn, is surface mounted onto a small custom design PCB. The use of a flex cable provides both strain relief and mechanical stability. In addition, the light weight of the connector (<35 mg) minimizes the physical load on the animal. The PCB includes a through hole terminal block from which the output is fed to a differential amplifier (Model 1700, AM Systems Inc., WA), which is connected to the data acquisition system. Fig. 3A shows the interconnection system between a microelectrode array and the PCB described above.

One main advantage of this interconnect configuration is the opportunity to replace devices with different array designs by simply unlocking the actuator of the ZIF connector. In a similar fashion, flex cables of different lengths can be interchanged. According to specific experimental requirements, the differential recording configuration of an array can be modified by changing the output wiring scheme of the terminal block that defines the electrode pairing. This is especially useful when different areas of a certain muscle need to be sampled or when the alignment of the recording sites with respect to the muscle fibers need to be modified.

2.5. Electrical characterization

The electrical integrity of the micro-fabricated probes was established before implantation. A continuity test was performed to ensure that each electrical path between a recording site and its corresponding terminal pad was complete and functional. An additional test was carried out to verify that the metal traces were not shorted to one another. The electrical performance of the electrodes was evaluated by impedance spectroscopy. Since the metal–electrolyte interface determines the impedance of the electrodes (McAdams et al., 1995; Geddes, 1997), measurements were taken keeping the shaft of the devices immersed in modified Miyazaki saline (Trimmer and Weeks, 1989) to mimic the physiological environment that surrounds the electrodes when implanted. A large silver/silver chloride pellet (1 mm × 2.5 mm, AM Systems Inc. WA) was used as a reference electrode. Through the outputs of the interconnecting PCB, the impedance of single recording sites was determined with an LCR meter (Agilent E4980A Precision LCR Meter) by recording the response to sinusoidal current pulses over the frequency range of 100–200 kHz. To monitor the recording capabilities of the electrodes over time, impedance measurements were taken before and after implantation at room temperature.

2.6. In vivo and in vitro testing

The ability of the devices to record electromyography activity was tested *in vivo* in 5th instar larvae of *M. sexta* (Fig. 3B). First, the animals were chilled on ice for 30 min. Next, using a pair of dissecting micro-scissors, an incision was made along the cuticle in correspondence of the target muscles. Holding it with a pair of fine tweezers, the electrode was fed into the cut with the recording sites facing inwards (to target external muscles) or outwards

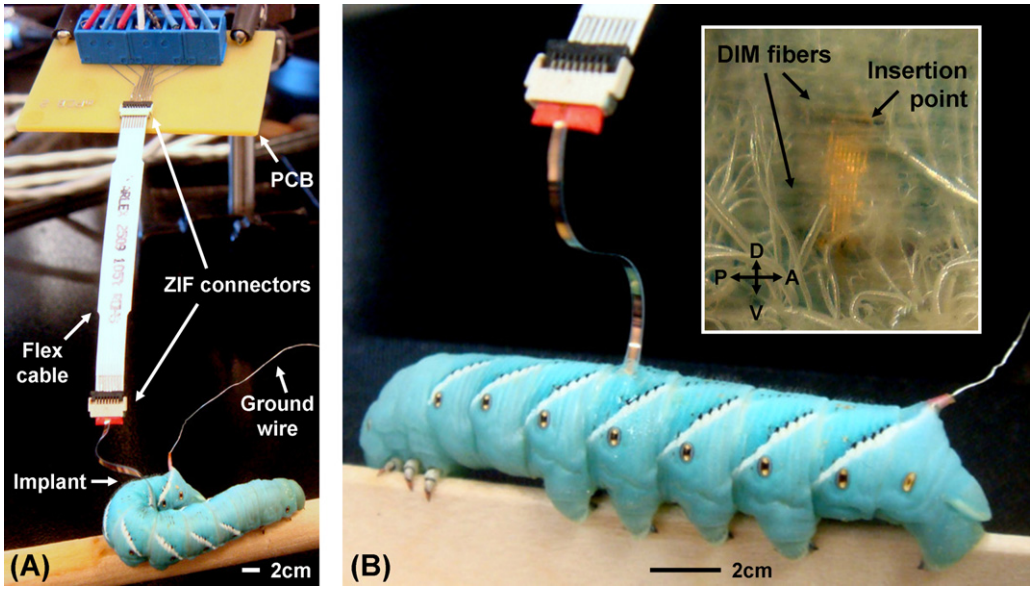

Fig. 3. Experimental setup and *in vivo* implantation. (A) The interconnection system described in Section 2.4 is shown during a recording session. The microdevice implanted in *Manduca* is connected to a flex cable through a ZIF connector. The flex cable is inserted into another ZIF connector soldered to a small PCB. The outputs of the PCB are fed into a differential amplifier. The flex cable shown here is 5.1 cm long but it is possible to connect cables of different lengths. The device is very flexible and its shank can twist and turn as the animal moves on a wooden stick. The PCB is mounted on a manipulator with a rigid arm that can be moved to follow the animal along the stick. The ground silver wire is inserted through the horn of the animal. (B) *Manduca* with a device implanted in the dorsal side of the fourth abdominal segment. After each recording session, the location of the electrode array is verified using the semi-intact preparation described in Section 2.6. A typical post-mortem dissection is shown in the inset. In this case, the array is positioned underneath the large longitudinal muscle DIM. The muscle fibers appear intact and no toxic reaction is observed. A – anterior, P – posterior, D – dorsal, V – ventral.

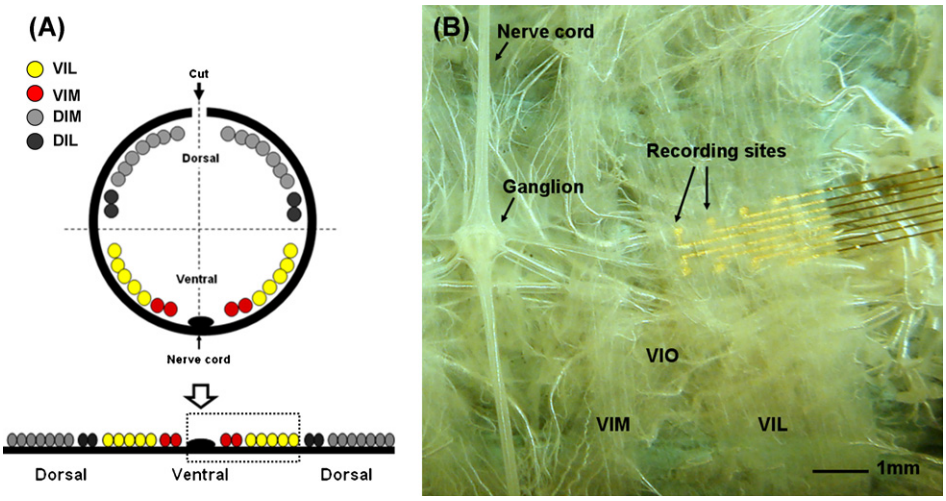

Fig. 4. Semi-intact preparation. (A) Schematic representation of how a semi-intact preparation (flaterpillar) is obtained. As shown by the cross section of *Manduca* body (top panel), when the cuticle is cut along the dorsal midline and pinned down, all the muscles flatten on a plane (bottom panel). Although the three dimensional arrangement of the muscles is lost, their relative position to each other is preserved. For simplicity, only the major dorsal and ventral muscles are shown. (B) View from above of a flaterpillar preparation, corresponding to the window in the bottom panel of (A). A micro-fabricated device is slid underneath the fibers of the ventral muscle VIL. The gold electrodes are facing upward to record from VIL. The ventral oblique muscles VIO and VEO can be seen crossing each other below the array. On the far left, the nerve cord and a ganglion are visible.

(to target internal muscles). It is only necessary to push gently, as the probe slides effortlessly in-between muscles. To avoid excessive hemolymph seepage, the cut on the cuticle was carefully made to approximate the width of the device. Finally, to keep the electrode array in place and seal the incision, a small amount of rubber cement (Elmer's Products Inc.) was distributed along the cut. A silver wire was inserted through the horn of the animal to act as a ground wire. After the insertion, animals recovered quickly (20 min) and seemed to tolerate the devices extremely well as they move and behave normally. Numerous post-mortem dissections have confirmed that the musculature is left intact by the sliding electrode and that there are no significant toxic reactions (Fig. 3B, inset). During the recording sessions, the animals were kept on a wooden rod and were free to move in any direction.

EMG signals were amplified at ×10,000, high-pass-filtered at 10 Hz, and low-pass-filtered at 10 kHz. Data was acquired using the WinDaq Pro software package (DataQ Instruments), while processing and spike sorting were performed offline with the freely available program DataView (www.st-andrews.ac.uk/~wjh/dataview/).

To assess the spatial sensitivity of the array, a semi-intact preparation (called flaterpillar) was used. As schematically illustrated in Fig. 4A, after making an incision along the cuticle, the larva was pinned down, with the ventral side up, to a Sylgard dish in cold modified Miyazaki saline (Trimmer and Weeks, 1989). Once the gut and most of the fat body were removed, the nerve cord and the musculature were left exposed (Fig. 4B). Since all the ganglia, nerves and muscles were left intact, excitatory junction potentials (EJP) could be recorded. Spontaneous muscle activity typically persists for up to 2 h after the animal is pinned down in saline. Data was acquired and processed as described in the case of the freely behaving animals.

The flaterpillar preparation was also used to verify the exact electrode location after each live recording session. A typical post-mortem dissection showing the electrode array underneath the large dorsal muscle DIM is presented in the inset of Fig. 3B.

3. Results

Flexible micro-electrode arrays were custom fabricated for *in vivo* EMG recordings in *M. sexta*, our animal system. They consist of a chrome/gold conductive layer sandwiched between two flexible insulating layers of parylene C. The geometry of the array has been specifically designed to match the anatomical features of the larval stage of *Manduca*. Eight circular recording sites of 50 μm radius terminate into eight 300 μm square bond pads through a set of metal traces encapsulated in parylene insulation. One of the final devices and a photomicrograph of the apertures that define the electrodes and the terminals are shown in Fig. 1. The exposed area of the gold electrodes has been designed to be slightly less than that patterned via photolithography to guarantee an effective parylene encapsulation (Fig. 1C). The final exposed area has been estimated to be 5500 μm^2.

The devices have been fabricated with different widths (700–1500 μm) and differing electrode spacing (500–1000 μm) to allow minimally invasive implantations in various parts of the animal – something especially important when targeting less accessible muscles. The 500 μm pitch of the terminal pads has been chosen to match that of a ZIF micro-connector. Through a flat flex cable soldered to this micro-connector, the probe is connected to a small PCB (Fig. 3A), whose outputs are fed to a differential amplifier. The electrodes are connected in a differential configuration that yields four final recording channels (Fig. 5, inset). To prevent motion artifacts due to wire-pulling, the PCB has been securely fixed to a manipulator with a rigid arm that can be moved both vertically and horizontally to follow the animal during a recording session (Fig. 3A).

The devices are thin (16–20 μm) and flexible, yet they are structurally robust and they do not buckle during insertion. They have been re-used several times obtaining consistent results.

When the array is implanted, a metal–electrolyte interface is established at each electrode site (Geddes, 1997). For this reason, a careful electrical characterization of the electrodes has been performed via impedance spectroscopy in modified Miyazaki saline (Trimmer and Weeks, 1989). Sixteen electrodes of two different devices have been examined before and after implantation. A typical value of $48 \pm 2\,k\Omega$ has been found at 1 kHz. No significant impedance drop has been observed after recording sessions of several hours. Not only the impedance is stable over time, but also uniform among the electrodes, a crucial requirement for an adequate differential amplification.The magnitude of the impedance of two electrodes constituting a recording channel is plotted in Fig. 5 as a function of the frequency. The two curves are nearly identical

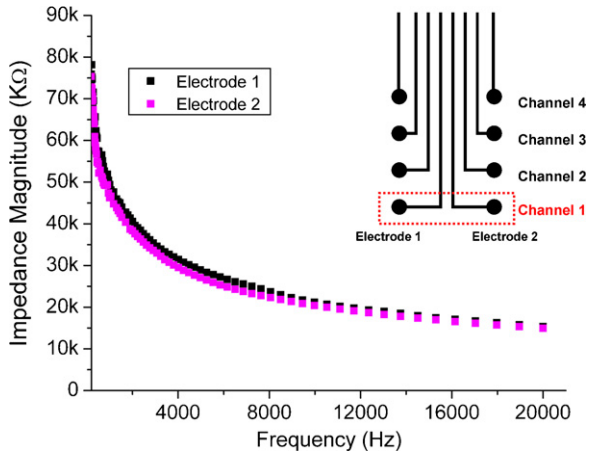

Fig. 5. Impedance and channel layout. The magnitude of the impedance of two electrodes constituting one recording channel (channel 1 in the inset) is shown as a function of the frequency. The two curves are nearly identical. At 1 kHz, the impedance of both electrodes is approximately 48 kΩ. The inset shows the four channel differential configuration used in the experiments described in Sections 3.1 and 3.2.

and mostly overlap in the whole frequency range. A more detailed evaluation of the electronic properties of the devices after longer term implantations is underway.

The recording capability of the micro-electrode arrays has been evaluated in *Manduca* both in vitro and *in vivo*.

3.1. In vitro results

The semi-intact preparation (flaterpillar) has been used to assess the spatial selectivity of the electrode array and the possible presence of artifacts due to motion. In fact, since the location of the recording sites can be easily seen through the transparent parylene C substrate, it is possible to strategically place the array on top of any muscle with extreme precision (Fig. 4B). This offers the opportunity to test for channel selectivity with a greater accuracy than when the device is implanted in an intact animal.

In the sets of experiments presented here spontaneous activity was recorded from the major ventral and dorsal muscles. Although spontaneous activity is random in nature and is not necessarily representative of any motor pattern, it constitutes a fast and easy way to study the recording capabilities of our device.

The electrode was first slid underneath the largest dorsal muscle (DIM) with the recording sites facing toward the oblique muscles, as exemplified in Fig. 6A. The two recording electrodes constituting channel 1 were placed on LIO, while those corresponding to channel 2 were placed on DIO. Channels 3 and 4 were positioned in proximity of DIO and DEM. EJP events were detected and sorted using threshold and cluster analysis (Fig. 6B). EJPs of each type were averaged ($n = 10–35$) to highlight how activities from different muscles are distributed among the four channels. Some EJPs were detected on all channels (Fig. 6B, panel (iii)), while others were selectively detected on individual channels: LIO activity is present only on channel 1 (Fig. 6B, panel (i)); DIO activity on both channels 1 and 2 (Fig. 6B, panel (ii)); and DEM activity on channels 3 and 4 (Fig. 6B, panel (iv)).

On the ventral side, the electrode was slid between VIL and VIO with the recording sites facing toward the oblique muscles VEO (channels 1, 2, and 4) and VIO (channel 3), as depicted in Fig. 7A. In spite of the overlapping nature of VIO and VEO, their individual muscle activities can be clearly identified across the four channels (Fig. 7B).

Averages of each type of EJPs ($n = 50–54$) detected by threshold analysis are also shown to illustrate how the amplitude and waveform of the EJPs recorded on each channel can be used to distinguish activity in different muscles: activity on channel 3 corresponds to

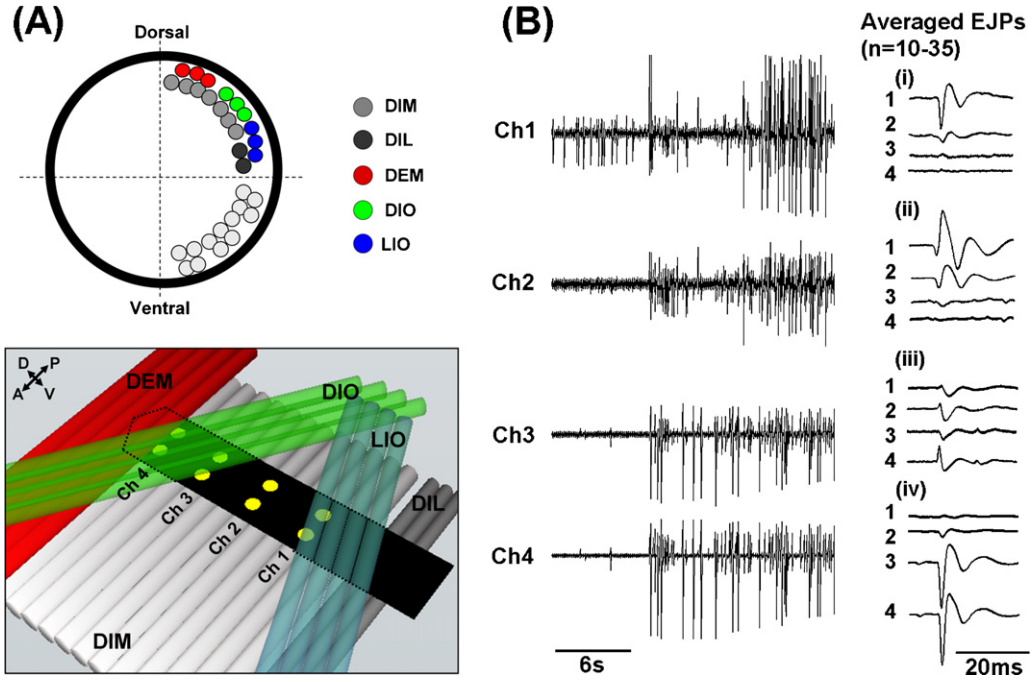

Fig. 6. In vitro results from dorsal muscles. Example of four-channel recordings of spontaneous EJPs from dorsal muscles in a semi-intact preparation. (A) Schematic representation of the position of the electrode array during the recording session: the device was inserted under DIM with the recording sites facing toward the longitudinal muscle DEM and the oblique muscles DIO and LIO. The cross section at the top shows how these muscles are arranged in an intact animal. (B) Spontaneous EJPs are observed on all the four channels. Using threshold and cluster analysis, EJPs were sorted into different subsets. The averages of 10–35 events of each type are shown in panels (i)–(iv). Some EJPs were detected on all channels (iii), but some were selectively detected on channel 1 (i), channels 1 and 2 (ii), and channels 3 and 4 (iv), presumably corresponding to LIO, DIO and DEM. In each panel, the voltage gain is the same for all channels. A – anterior, P – posterior. Muscle acronyms by position: D – dorsal, V – ventral, L – lateral, M – medial; by layer E – external, I – internal; and by angle: O – oblique.

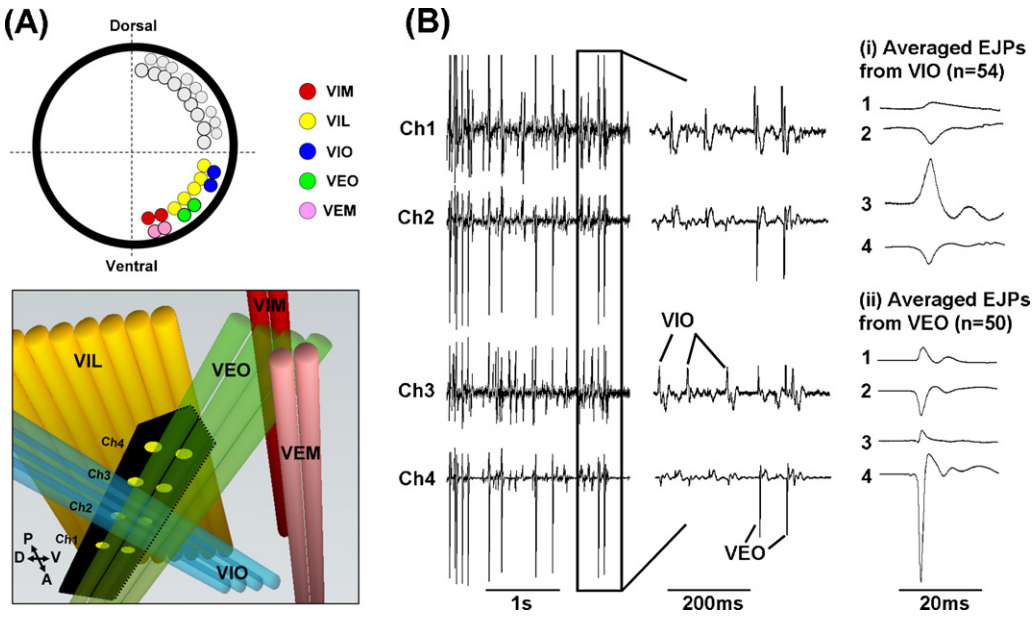

Fig. 7. In vitro results from ventral muscles. Example of four-channel recordings of spontaneous EJPs from ventral muscles in a semi-intact preparation. (A) Schematic representation of the position of the electrode array during the recording session: the device was inserted between VIL and VIO, with the recording sites facing toward the oblique muscles VEO (channels 1, 2, and 4) and VIO (channel 3). The cross section at the top illustrates how these muscles are arranged in an intact animal. (B) EJPs detected on the four channels are shown in two time scale. The traces in panels (i) and (ii) represent the averages of the EJPs triggered by VIO and VEO and sorted by threshold analysis. VIO is mainly detected on channel 3, while VEO is mainly detected on channel 4. In each panel, the voltage gain is the same for all channels. A – anterior, P – posterior. Muscle acronyms by position: D – dorsal, V – ventral, L – lateral, M – medial; by layer E – external, I – internal; and by angle: O – oblique.

VIO (Fig. 7B, panel (i)), while activity on channel 4 corresponds to VEO (Fig. 7B, panel (ii)).

By moving the array with respect to the surrounding muscles, it was also possible to evaluate the effect of micro-motion on the recorded waveforms. We found that these effects are minimal as most slow movements (possibly due to internal motions of the soft body when the electrode is implanted *in vivo)* can be effectively filtered out using a 10 Hz high pass filter.

3.2. *In vivo results*

The device was implanted in 5th larval instars of *Manduca*. An incision was made on the dorsal side of abdominal segment A4 posterior to the spiracle (Fig. 8A). Since the relative positions of all the major muscles within an abdominal segment have been previously mapped to external features of the body surface, it was possible to place the array in the desired recording configuration by simply sliding it perpendicularly to the cut with the electrode pads facing outwards. In particular, by knowing the length of the shank inserted into the animal and by knowing the longitudinal and transverse spacing between the electrodes, single channels can be placed very close to the desired muscles. A post mortem dissection confirmed the exact location of the array, as described in Section 2.6.

In the first set of experiments, recordings were performed during vigorous side-to-side casting behavior, evoked by pinching alternatively on the left and on the right side of the terminal segment. EJPs from different dorsal muscles (DIL, DIO, and LIO) were selectively detected across the four channels (Fig. 8B). A high signal to noise ratio and the absence of movement artifacts characterize the recordings. Furthermore, left and right casting movements exhibit distinct motor patterns. The onset of activity in different muscles is clearly evident. DIO and LIO are active throughout the

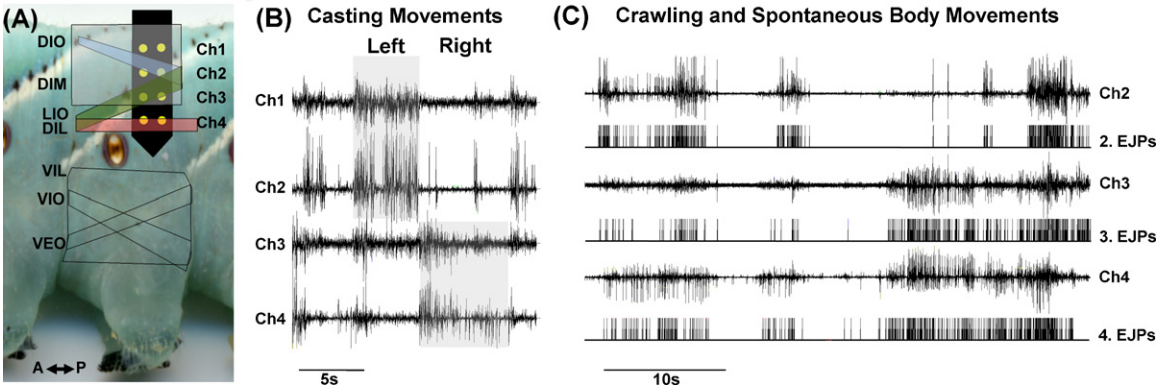

Fig. 8. *In vivo* results. Examples of EMG recordings in intact *Manduca*. (A) Major muscles on one side of an abdominal segment mapped to external features showing the position of an inserted array. Channels 1 and 2 were located in proximity of DIO, while channels 3 and 4 were positioned in correspondence of LIO and DIL, respectively. (B) Four-channel recordings during vigorous side-to-side casting behavior demonstrate muscle selectivity and absence of movement artifacts. (C) Channel recordings of crawling and general body movements with EJP events identified from the traces and marked below each record. The events can be parsed further into channel-specific motor patterns. A – anterior, P – posterior. Muscle acronyms by position: D – dorsal, V – ventral, L – lateral, M – medial; by layer E – external, I – internal; and by angle: O – oblique.

movement to the left (channels 1 and 2) but not during movement to the right (channels 3 and 4). DIL exhibits most activity when the animal turns to the right, ipsilateral to the electrode.

During the same recording session, the animal also performed a series of crawls accompanied by spontaneous body movements. Fig. 8C shows the recording corresponding to one of these crawls. Activity detected on channel 2 through 4 consisted of coordinated bursts corresponding to stepping movements. Although several muscles were coactive, their individual electrical responses were clearly discriminated on each channel. This activity could be defined as separate EJP events to reveal patterns of motor neuron firing during each type of movement. These recordings provide much finer discrimination of muscle activity than is currently available using fine wires (Simon et al., 2010). A comprehensive series of experiments is currently underway to understand how such motor patterns relate to specific movements.

4. Discussion

Any recorded EMG signal is a convoluted, non-stationary signal. In general, it is affected not only by the intricate muscle anatomy and the physiological and biochemical properties of neuromuscular transmission, but also by the performance characteristics of the instrumentation used to collect the signals (De Luca, 2006; Reaz et al., 2006). To improve the overall quality of the recordings, the functional capabilities of any EMG device can be enhanced by maximizing three main factors: (1) signal to noise ratio, (2) signal discrimination, and (3) signal stability. Here we present a minimally invasive microdevice intended for multichannel EMG recordings. To minimize signal distortion due to motion artifacts, a highly flexible polymer (parylene C) has been selected as the structural substrate to allow a more conformal coverage of the muscle surface. The final device is not only extremely thin (<20 μm) and flexible, but also mechanically robust, dimensionally stable and biocompatible.

To allow precise positioning and optimize its signal detection capabilities, the size and the overall design of the micro-electrode array have been specifically customized to suit the anatomical features of our model animal, the tobacco hornworm *M. sexta*. Because the SNR is almost entirely determined by the properties of the electrode interface, a careful electrical characterization was performed to ensure that the value of the impedance is not only consistent over time, but also does not vary among the recording sites of the array.

The current design is suitable to record from the vast majority of *Manduca* muscles. We plan to employ the same fabrication protocol to produce devices with slightly different design parameters in order to target less accessible muscle groups as well. More generally, the number of recording channels, the electrode detection area and inter-site distances can be easily modified to meet the requirements for EMG recordings in other animal systems, both vertebrates and invertebrates.

Preliminary recordings in freely moving *Manduca* exhibit excellent signal to noise ratio, no significant motion artifacts, good channel discrimination of individual muscle activities, and EJP amplitudes and waveforms highly consistent over time. The animals tolerated the microdevice extremely well and exhibited natural behaviors for the whole duration of each recording session (up to 5 h).

Motor activities can be unambiguously assigned to distinct muscles by capitalizing on the fact that individual channels are highly selective to different muscles but not entirely specific to one muscle. Since a single channel detects EJPs from the closest muscles with the highest selectivity, the amplitude of the EJPs corresponding to any given muscle will vary across the four channels proportionally to the distance between each channel and that particular muscle. At the same time, however, the amplitude of the EJPs from any muscle remains constant over time on each channel, allowing individual motor unit activities to be resolved within each channel recording. Therefore, by cross-correlating the motor units identified in each channel and comparing their amplitudes, it is possible to match motor activities to individual muscles with high precision. When channel-specific motor patterns are superimposed, the overall motor pattern associated with a particular behavior can be identified (Fig. 8).

While activities from small muscles tend to appear only in one or two channels, EJP events from bigger muscles are likely to be present in more than two channels. Using the current four channel configuration, a minimum of two muscles can be typically recorded simultaneously – a performance already superior to that of traditional bipolar wire electrodes.

Arrays with a larger number of more closely spaced electrodes are expected to resolve more than two muscles at the same time. Furthermore, since the quality of the recordings strongly depends on the amplification process, future plans include an additional signal conditioning step via the use of a preamplifier to further improve the SNR.

In conclusion, the microelectrode array presented here offers the unique opportunity to simultaneously record motor activity from different muscles in freely behaving *M. sexta*, overcoming the experimental limitations of traditional stiff wire electrodes and potentially simplifying the acquisition of muscle activation sequences underling motor control and motor coordination. By varying basic design parameters, we envision its application not to be limited to soft bodied animals but span a wide range of small animal species where probe flexibility represents a major advantage.

Acknowledgments

CM would like to thank all the members of the Tufts Micro and Nanofabrication Facility for their help. This work was funded by the National Science Foundation grant IOS 0718537 to BAT.

References

Ahn AN, Full RJ. A motor and a brake: two leg extensor muscles acting at the same joint manage energy differently in a running insect. J Exp Biol 2002;205:379–89.
Ahn AN, Meijer K, Full RJ. In situ muscle power differs without varying in vitro mechanical properties in two insect leg muscles innervated by the same motor neuron. J Exp Biol 2006;209:3370–82.
Ayers JL, Davis WJ. Neuronal control of locomotion in the lobster, *Homarus americanus*. J Comp Physiol A 1977;115:1–27.
Belanger JH, Trimmer BA. Combined kinematic and electromyographic analyses of proleg function during crawling by the caterpillar *Manduca sexta*. J Comp Physiol A 2000;186:1031–9.
Buchthal F, Guld C, Rosenfalck P. Multielectrode study of the territory of a motor unit. Acta Physiol Scand 1957;39:83–104.
Chiel HJ, Ting LH, Ekeberg O, Hartmann MJZ. The brain in its body: motor control and sensing in a biomechanical context. J Neurosci 2009;29:12807–14.
Clarac F, Pearlstein. Invertebrate preparations and their contribution to neurobiology in the second half of the 20th century. Brain Res Rev 2007;54(1):113–61.
De Luca CJ. Electromyography. In: Webster JG, editor. Encyclopedia of Medical Devices and Instrumentation. second ed. New York: John Wiley; 2006.
Dickinson MH, Farley CT, Full RJ, Koehl MA, Kram R, Lehman S. How animals move: an integrative view. Science 2000;288:100–6.
Farina D, Yoshida K, Stieglitz T, Koch KP. Multichannel thin-film electrode for intramuscular electromyographic recordings. Appl Physiol 2008;104:821–7.
Geddes LA. Historical evolution of circuit models for the electrode-electrolyte interface. Ann Biomed Eng 1997;25(1):1–14.
Gielen SC. What does EMG tell us about muscle function? Motor Control 1999;3:9–11.
HajjHassan M, Chodavarapu V, Musallam S. NeuroMEMS: neural probe microtechnologies. Sensors 2008;8(10):6704–26.
Herold KE, Rasooly A, editors. Lab-on-a-Chip Technology: Fabrication and Microfluidics. Norfolk, UK: Caister Academic Press; 2009. p. 333–51.
Hillel AD. The study of laryngeal muscle activity in normal human subjects and in patients with laryngeal dystonia using multiple fine-wire electromyography. Laryngoscope 2001;111(4 Pt 2 Suppl. 97):1–47.

Huxley AF. Cross-bridge action: present views, prospects, and unknowns. J Biomech 2000;33:1189–95.
Jayne BC. Muscular mechanisms of snake locomotion, an electromyographic study of lateral undulation of the Florida banded water snake (*Nerodia fasciata*) and the yellow rat snake (*Eiaphe obsoieta*). J Morphol 1988;197(2):159–81.
Jayne BC, Lauder GV. Are muscles fibers within fish myotomes activated synchronously? Patterns of recruitment within deep myomeric musculature during swimming in Largemouth Bass. J Exp Biol 1995;198:805–15.
Kar DC. Design of statically stable walking robot: a review. J Robotic Syst 2003;20:671–86.
Levine RB, Truman JW. Dendritic reorganization of abdominal motoneurons during metamorphosis of the moth, *Manduca sexta*. J Neurosci 1985;5:2424–31.
Licari JJ. Coating Materials for Electronic Applications: Polymers, Processing, Reliability, Testing. New York: Noyes Publication; 2003. pp. 154–167.
Lockhart DB, Ting LH. Optimal sensorimotor transformations for balance. Nat Neurosci 2007;10:1329–36.
Loeb GE, Bak MJ, Schmidt EM. Parylene as a chronically stable, reproducible microelectrode insulator. IEEE Trans Biomed Eng 1977;24(2):121–8.
Marsh RL. How muscles deal with real-world loads: the influence of length trajectory on muscle performance. J Exp Biol 1999;202(23):3377–85.
McAdams ET, Lackermeier A, McLaughlin JA, Macken D, Jossinet J. The linear and non-linear electrical properties of the electrode-electrolyte interface. Biosens Bioelectron 1995;10:67–74.
Nishikawa K, Biewener AA, Aerts P, Ahn AN, Chiel HJ, Daley MA, Daniel TL, Full RJ, Hale ME, Hedrick TL, Lappin AK, Nichols TR, Quinn RD, Satterlie RA, Szymik B. Neuromechanics: an integrative approach for understanding motor control. Integr Comp Biol 2007:1–39.
Reaz MB, Hussain MS, Mohd-Yasin F. Techniques of EMG signal analysis: detection, processing, classification and applications. Biol Proc Online 2006;8:11–35.
Rheuben MB. Degenerative changes in the muscle fibers of *Manduca sexta* during metamorphosis. J Exp Biol 1992;167:91–117.
Richardson Jr RR, Miller JA, Reichert WM. Polyimides as biomaterials: preliminary biocompatibility testing. Biomaterials 1993;14(8):627–35.
Rodger DC, Fong AJ, Li W, Ameri H, Ahuja AK, Gutierrez C, Lavrov I, Zhong H, Menon PR, Burdick EMJW, Roy RR, Edgerton R, Weiland JD, Humayun MS, Tai YC. Flexible parylene-based multielectrode array technology for high-density neural stimulation and recording. Sens Actuators B: Chem 2008;132(2):449–60.
Simon MA, Fusillo SJ, Colman K, Trimmer BA. Motor patterns associated with crawling in a soft-bodied arthropod. J Exp Biol 2010;213:2303–9.
Schmidt EM, McIntosh JS. Long-term implants of parylene C coated microelectrodes. Med Biol Eng Comput 1988;26:96–101.
Spence AJ, Neeves KB, Murphy D, Sponberg S, Land BR, Hoy RR, Isaacson MS. Flexible multielectrodes can resolve multiple muscles in an insect appendage. J Neurosci Methods 2007;159:116–24.
Subbaroyan J, Martin DC, Kipke DR. A finite-element model of the mechanical effects of implantable microelectrodes in the cerebral cortex. J Neural Eng 2005;2:103–13.
Ting LH, Macpherson JM. A limited set of muscle synergies for force control during a postural task. J Neurophysiol 2005;93:609–13.
Trimmer BA, Issberner JI. Kinematics of soft-bodied, legged locomotion in *Manduca sexta* larvae. Biol Bull 2007;212:130–42.
Trimmer BA, Weeks JC. Effects of nicotinic and muscarinic agents on an identified motoneurone and its direct afferent inputs in larval *Manduca sexta*. J Exp Biol 1989;144:303–37.
Voldman J, Gray LG, Schmidt MA. Microfabrication in biology and medicine. Annu Rev Biomed Eng 1995;1:401–25.
Vitti M, Basmajian JV. Integrated actions of masticatory muscles: simultaneous EMG from eight intramuscular electrodes. Anat Rec 1977;187(2):173–89.
Whelan PJ. Electromyogram recordings from freely moving animals. Methods 2003;30:127–41.
Wise KD. Silicon microsystems for neuroscience and neural prostheses. IEEE Eng Med Biol Mag 2005;24:22–9.
Woods J WA, Fusillo S, Trimmer BA. Dynamic properties of a locomotory muscle of the tobacco hornworm *Manduca sexta* during strain cycling and simulated crawling. J Exp Biol 2008;211:873–82.